Graph-Driven Domain Co-Adaptation for Cross-Domain Image Quality Assessment

Shun Zhu[1], Xichen Yang[1], Yan Zhang[1], Tianshu Wang[2], Zhongyuan Mao[1], Tianyin Li[1], Zhuoyan Sun[1], Xiaobo Shen[3]

[1]School of Computer and Electronic Information/Artificial Intelligence, Nanjing Normal University, Nanjing, China
[2]College of Artificial Intelligence and Information Technology, Nanjing University of Chinese Medicine, Nanjing, China
[3]School of Computer Science and Engineering, Nanjing University of Science and Technology, Nanjing, China
{shunzhu, xichen_yang, 19210424, zhongyuanmao, 2351525602, 242212033}@njnu.edu.cn, wangtianshu@njucm.edu.cn, njust.shenxiaobo@gmail.com

Abstract

As a typical information medium, images are widely utilized across various scenarios. Measuring image quality accurately is meaningful for the subsequent usability of images. However, significant variations exist in image types and distortion types in different scenarios. And, acquiring labeled images for each specific scenario is time-consuming and labor-intensive. Consequently, designing cross-domain image quality assessment (IQA) that generalizes across different scenarios remains a substantial challenge. Existing cross-domain IQA methods primarily focus on content relevance while neglecting distortion differences, leading to limited applicability while distortion fluctuates. To address these limitations, a graph-driven domain co-adaptation framework for cross-domain IQA (GDCIQA) is proposed. Firstly, a graph knowledge sharing (GKS) module that constructs graphs via inter-domain distortion relevance has been proposed. GKS employs graph neural networks to update quality-aware features in the source domain by leveraging target-domain representations. Secondly, the proposed co-adaptation learning (CAL) mechanism can enable joint optimization of different modules, which ensures comprehensive sharing of quality-aware and distortion-related information. Finally, a domain adaptation framework has been designed to train models effectively on labeled source images, yielding target-domain-optimized IQA models. Experimental results demonstrate that GDCIQA achieves higher accuracy and stability in cross-domain scenarios. The proposed GKS and CAL can advance cross-domain IQA research.

Code — https://github.com/dart-into/GDCIQA

Introduction

As a typical information medium, images can achieve efficient information transmission. Thus, images are widely applied in different scenarios. In the process of image acquisition, generation, transmission, and storage, distortions are inevitable due to different environments and technologies. This situation seriously affects the readability and application value of the image. Therefore, image quality assessment (IQA) (Yu et al. 2025; Min et al. 2025) is meaningful to improve the subsequent usability of images. However, the image types in real-world scenarios involves natural scenarios (Ghadiyaram and Bovik 2015), underwater scenarios (Jiang et al. 2022), AI generation (Fang et al. 2025). Meanwhile, the distortion type is various, which causes difference of quality assessment criteria. Most existing non-reference IQA (NRIQA) methods (Zhu et al. 2020; Liu et al. 2022) rely on the labeled images. And, acquiring labeled images for each specific scenario is time-consuming and labor-intensive. These IQA methods mainly focus on single scenario, which results in low performance in cross-doman tasks. Thus, it is significant to propose cross-domain IQA methods for distorted images in various scenarios.

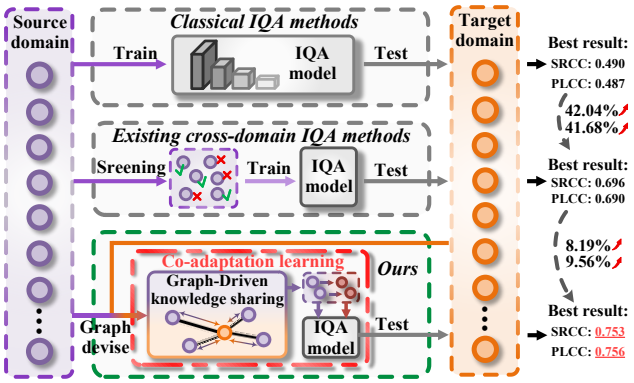

Figure 1: Effectiveness of information sharing between KADID and LIVEC. GDCIQA has obvious advantage over existing methods.

Recently, some cross-domain IQA methods (Lu et al. 2024; Li et al. 2024a; Hu et al. 2023; Lu et al. 2024; Chen et al. 2021a; Ajakan et al. 2014) have been proposed. Some studies (Li et al. 2024a; Hu et al. 2023) have demonstrated that generalizing all images of synthetically distorted dataset KADID (Lin, Hosu, and Saupe 2019) and TID2013 (Ponomarenko et al. 2013) to authentically distorted dataset LIVEC (Ghadiyaram and Bovik 2015) has negative performance. The outlier samples cause negative transfer of the model. DGQA (Li et al. 2024a) further screen subset of the source domain suitable for target domain through a distortion classification model. However, the model is limited to

the lack of target domain information analysis when trains on the source domain. To offer more effective information of the target domain for the model, several methods (Lu et al. 2024; Chen et al. 2021a; Ajakan et al. 2014) provide feedback information related to the target domain. StyleAM (Lu et al. 2024) feeds back the loss of domain recognition to the IQA model for better transfer. RankDA (Chen et al. 2021a) enriches the types of feedback information for more comprehensive adjustment to the target domain. These methods mostly consider the quality fluctuation, lacking a comprehensive consideration of the distortion differences. The analysis (Li et al. 2024a) of the distortion information is significant to IQA tasks. Considering distortion information sharing between the source domain and target domain may better address domain IQA tasks.

It is meaningful to propose effective methods for distortion information sharing between the source domain and target domain. As a classic information sharing instrument, the graph neural networks (GNNs) are mature in the application (Jin et al. 2024; Zhang 2025; Yang et al. 2025; Wang et al. 2024) of computer vision. The special structure of GNNs ensures dynamically processing node features and edge features. Thus, many GNNs-based methods (Zhang et al. 2023b; Li et al. 2022) can effectively enhance the representation of features. Employing GNNs to IQA methods can achieve information sharing between the source domain and target domain for feature enhancement. As illustrated in Figure 1, by employing GNNs for information sharing between the source domain and target domain, the performance is at least 8.19% and 9.56% higher than existing methods in SRCC and PLCC, respectively.

Moreover, the learning and updating patterns of IQA models require new adjustments, when other assistance modules are added. Several methods (Agnolucci et al. 2024; Guan et al. 2017) mainly consider the updating of IQA models, which causes slight update of distortion classification modules. LIQE (Zhang et al. 2023a) and SDD-FIQA (Ou et al. 2021) pay attention to both IQA models and the assistant modules. However, these methods manly guided the model to update for single scenarios, which fail to meet the cross-domain IQA tasks of various scenarios. In conclusion, co-adaptation learning for both IQA models and assistance modules is needed to face more various scenarios.

Based on the above conclusions, this paper proposes a graph-driven domain co-adaptation framework for cross-domain IQA (GDCIQA). Firstly, a graph knowledge sharing (GKS) module that constructs graphs via inter-domain distortion relevance has been proposed. GKS employs graph neural networks to update quality-aware features in the source domain by leveraging target-domain representations. Secondly, the proposed co-adaptation learning (CAL) mechanism can enable joint optimization of different modules, which ensures comprehensive sharing of quality-aware and distortion-related information. Finally, a domain adaptation framework has been designed to train models effectively on labeled source images, yielding target-domain-optimized IQA models. Experimental results demonstrate that GDCIQA achieves higher accuracy and stability in cross-domain scenarios. The proposed GKS and CAL can advance cross-domain IQA research. Our work contributions are summarized as follows.

- A GKS module is proposed to update the inter-domain features, which construct the graphs by fusing distortion-related and quality-aware information.
- A CAL mechanism is proposed to update parameters for different modules, which can meet the requirements of target domains in various scenarios.
- Experimental results demonstrate that GDCIQA achieves enhanced accuracy and stability in cross-domain IQA tasks.

Related Work

NRIQA

The scenarios (Li et al. 2019; Ghadiyaram and Bovik 2015; Li et al. 2023) in the real world faced by IQA are various. The different image types and distortion types result in difference in quality assessment criteria. Thus, it is a challenge for IQA to address cross-domain tasks, which are related to various application scenarios.

Most existing IQA methods (Hu et al. 2023; Zhang et al. 2024; Ke et al. 2021) focus on the performance in single scenarios. While addressing unlabeled cross-domain tasks, the performance of these methods is not satisfactory. Many deep-learning-based NRIQA methods (Zhang et al. 2023a; Hu et al. 2025) have been proposed to meet more distorted images types. Su et al. (Su et al. 2020) proposed an adaptive hyper network, which perceives more quality evaluation rules. Zhang et al. (Zhang et al. 2023a) designed a DB-CNN to improve the accuracy of feature extraction by using a double-stream neural network. Zhu et al. (Zhu et al. 2020) utilized meta-learning to learn the quality information of different distorted images. These methods can only meet the requirement of specific scenarios.

To improve the performance in cross-domain tasks, some cross-domain IQA methods (Liu et al. 2022; Li et al. 2024a) have been proposed. Some studies (Li et al. 2024a; Hu et al. 2023) have demonstrated that the outlier samples in the source domain may cause negative transfer. Thus, some cross-domain IQA methods (Li et al. 2024a; Chen et al. 2021b) screen source domain images by alignment methods and metric methods. DGQA (Li et al. 2024a) obtains a sub-domain by aligning the distortion type distribution between the source and target domains. In UCDA (Chen et al. 2021b), the samples of the target domain are divided into confident and non-confident sub-domains to realize the alignment of the source domain. However, the complex difference of in style and distortion information between the source domain and the target domain needs a more comprehensive analysis. More information interaction between the source domain and the target domain should be taken into account.

Considering the above conclusions, the complexity of cross-domain IQA tasks also requires strategy for feature interactions and knowledge sharing between the source domain and the target domain.

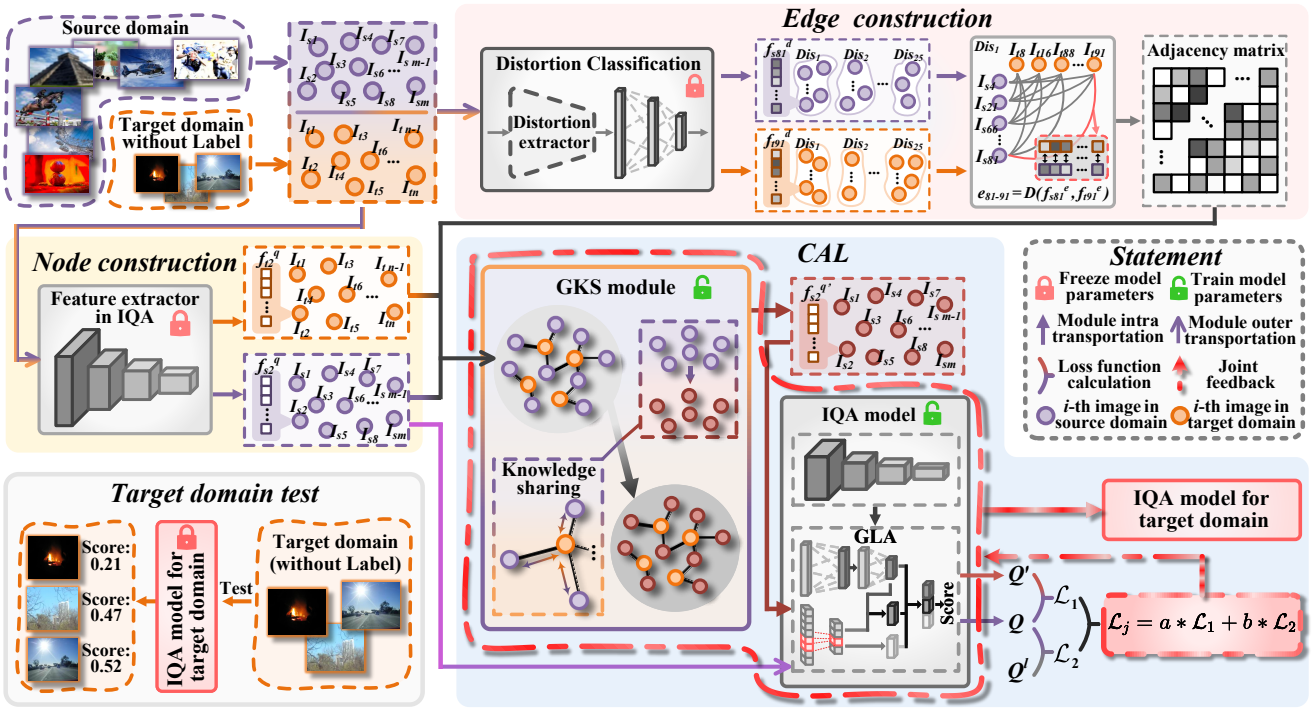

Figure 2: The illustration of GDCIQA.

GNNs

Classical GNNs methods (Zhuo et al. 2025a,b) can utilize the information of neighborhood nodes to optimize features. This ability can enhance the model understanding ability in graph data. With the application scenarios of GNNs rich, more feature enhancement methods based on GNNs (Zhang et al. 2023b; Li et al. 2022; Fang et al. 2023; Yang et al. 2024) have been expanded. KANO (Fang et al. 2023) and KGPLMs (Yang et al. 2024) utilize GNNs for feature enhancement, which significantly enhances the expressiveness of features, and then improve the accuracy of models.

Due to the advantages of feature enhancement and update, GNNs are widely used in computer vision(Jin et al. 2024). The related scenarios involve graph generation (Im et al. 2024), visual reasoning (Wei et al. 2024), etc. KerPrint (Yang et al. 2023) and GEST (Cheng, Liu, and Zeng 2023) enhance the features expression by knowledge graph. These graph mechanisms greatly improves the accuracy of the model. Considering the various scenarios that IQA meets, utilizing GNNs for feature optimization in IQA tasks is feasible. However, the research of GNNs-based IQA still needs more exploration. GraphIQA (Sun et al. 2022) uses distortion type and level as the basis for constructing edges. This method only focuses on the single IQA scenario, which neglects the application of GNNs on cross-domain tasks. Thus, effectively employing GNNs for cross-domain IQA tasks is still a challenge.

Considering the above conclusions, employing GNNs to IQA for feature update can share knowledge between the source domain and target domain. In this way, IQA methods can be adaptively optimized for various scenarios.

Method

GDCIQA consists of quality-aware and distortion-related features extraction, graph-driven feature update, and co-adaptation learning. The overall structure of GDCIQA is illustrated in Figure 2.

Feature Extraction

GDCIQA uses an IQA model $\mathcal{G}_{IQA}$ and a distortion classification model $\mathcal{G}_{DC}$ for extracting quality-aware features and distortion-related features, respectively.

$\mathcal{G}_{IQA}$ consists of a feature extractor $\mathcal{G}_{fex}$ and a global and local analysis (GLA) module $\mathcal{G}_{gla}$. Swin Transformer (Liu et al. 2021) is employed as feature extractor due to great ability of semantics analysis. $\mathcal{G}_{IQA}$ trains on the KADID and the parameters of $\mathcal{G}_{fex}$ are frozen. The distorted image I is input to obtain quality-aware feature f^q.

$\mathcal{G}_{DC}$ consists of a distortion extractor and a semantic layer. ResNet-50 (Targ, Almeida, and Lyman 2016) is employed as distortion extractor due to great ability of feature analysis. The semantic layer consists of linear layers of 1000-256-25. Batch normalizations are added after linear layers. $\mathcal{G}_{DC}$ trains on the KADID and the parameters are frozen. The distorted image I is input to obtain distortion-related feature f^d and distortion type $dis_z, z \in (1, 25)$.

Graph-Driven Feature Update

GDCIQA uses quality-aware features and distortion-related features of the source domain and target domain to construct

graph features. Then, the GKS module analyzes the graph features for knowledge sharing and feature update.

The images in source domain $\mathcal{D}om_s$ and target domain $\mathcal{D}om_t$ are defined as $\{I_{si}, i \in (1,m)\}$ and $\{I_{tj}, j \in (1,n)\}$, respectively. $\{I_{si}, i \in (1,m)\}$ and $\{I_{tj}, j \in (1,n)\}$ are input to $\mathcal{G}_{DC}$ for distortion-related features $\{f_{si}^d\}$ and $\{f_{tj}^d\}$. The distortion-related similarity $\mathcal{D}(f_{si}^d, f_{tj}^d)$ between the source domain image I_{si} and the target domain image I_{tj} within the same dis_i is as follows.

$$\mathcal{D}(f_{si}^d, f_{tj}^d) = \sqrt{(v_{si} - v_{tj})^T (\frac{co_{si} - co_{tj}}{2})^{-1} (v_{si} - v_{tj})}, \tag{1}$$

where v_{si} and v_{tj} represent the mean vectors of f_{si}^d and f_{tj}^d, respectively, and co_{si} and co_{tj} represent the covariance matrices of f_{si}^d and f_{tj}^d, respectively. $D(f_{si}^d, f_{tj}^d)$ is set as the edge $e_{i,j}$ between I_{si} and I_{tj}. The adjacency matrix $\mathcal{A}_{st}$ consisting of all edges is as follows.

$$\mathcal{A}_{st} = \{e_{i,j} = \mathcal{D}(f_{si}^d, f_{tj}^d) | i \in (1,m), j \in (1,n)\}. \tag{2}$$

The quality-aware features f_{si}^q and f_{tj}^q obtained by $\mathcal{G}_{IQA}$ are employed as node features of I_{si} and I_{tj}, respectively. The whole node feature matrix $\mathcal{H}_{st}$ is as follows.

$$\mathcal{H}_{st} = \{\{f_{si}^q\}, \{f_{tj}^q\} | i \in (1,m), j \in (1,n)\}. \tag{3}$$

The GKS module is used for updating $\mathcal{H}_{st}$ according to $\mathcal{A}_{st}$, which consists of two graph convolutions and activation function σ. The update process in the first graph convolution is as follows:

$$\mathcal{H}_{st}^{'} = \sigma(\mathcal{A}_{st}\mathcal{H}_{st}\mathcal{W}_1 + \mathcal{B}_1), \tag{4}$$

where $\mathcal{H}_{st}^{'}$ and $\mathcal{W}_1$ represent the updated node feature matrix and weight matrix of the first graph convolution, respectively. $\mathcal{B}_1$ represents the bias matrix. After analyzed by two graph convolutions, the updated node feature matrix $\mathcal{H}_{st}^{''}$ is obtained. The updated source domain node feature $\{f_{si}^{q''}\}$ is separated from $\mathcal{H}_{st}^{''}$. The process of graph-driven feature update is described in Algorithm 1.

Co-Adaptation Learning

GDCIQA uses the GLA module $\mathcal{G}_{gla}$ to obtain quality scores of $\{f_{si}^q\}$ and $\{f_{si}^{q''}\}$. The loss feedback information calculated by different scores and labels is for joint update.

$\mathcal{G}_{gla}$ uses linear layers and one-dimensional convolution (1DCNN) to obtain the global semantic feature f_g and local semantic feature f_l, respectively. A cross-attention mechanism is used to obtain cross-semantic feature from f_g and f_l. The fusion semantic feature f_{fusion} containing f_g, f_l, and cross-semantic feature is as follows.

$$f_{fusion} = f_g \oplus f_l \oplus att(f_g, f_l), \tag{5}$$

where $\oplus$ and att represent channeled concatenated and cross-attention mechanism, respectively. Then, a linear layer is used to map f_{fusion} for the quality score.

The difference between $\{f_{si}^q\}$ and $\{f_{si}^{q''}\}$ is analyzed for loss feedback, which guides the model to transfer to the target domain. Specifically, $\{f_{si}^q\}$ and $\{f_{si}^{q''}\}$ are input to the GLA module to obtain corresponding quality scores $\mathcal{Q}_{si}^{'}$ and $\mathcal{Q}_{si}$, respectively. The difference between $\mathcal{Q}_{si}$ and $\mathcal{Q}_{si}^{'}$ is calculated as loss information $\mathcal{L}_1$:

$$\mathcal{L}_1 = \sum_{i=1}^{m} \left\| \mathcal{Q}_{si} - \mathcal{Q}_{si}^{'} \right\|^2. \tag{6}$$

The distance between labels $\{\mathcal{Q}_{si}^l\}$ and the source domain is also part of loss feedback information, which balance the model for better fusing the target domain and the source domain. The difference between Q_{si} and label score $\mathcal{Q}_{si}^l$ is calculated as loss information $\mathcal{L}_2$:

$$\mathcal{L}_2 = \sum_{i=1}^{m} \left\| \mathcal{Q}_{si} - \mathcal{Q}_{si}^{l} \right\|^2. \tag{7}$$

The CAL aims to avoid the GKS module inevitably overly focusing on the information of the target domain, when guiding the model to transfer to the target domain. Thus, the joint feedback information $\mathcal{L}_j$ which contains $\mathcal{L}_1$ and $\mathcal{L}_2$ is employed.

$$\mathcal{L}_j = a * \mathcal{L}_1 + b * \mathcal{L}_2, \tag{8}$$

where a and b represent the weight of $\mathcal{L}_1$ and $\mathcal{L}_2$. $\mathcal{L}_j$ is used as jointly feedback to update the GKS module and the IQA model. The IQA model parameter θ_{IQA} is updated towards the quality fluctuation law suitable for the target domain. The update process of θ_{IQA} and θ_{GKS} is as follows:

$$\theta_{IQA}^{'} = \theta_{IQA} - \eta * \nabla_{\theta_{IQA}} \mathcal{L}_j(\theta_{IQA}), \tag{9}$$

$$\theta_{GKS}^{'} = \theta_{GKS} - \eta * \nabla_{\theta_{GKS}} \mathcal{L}_j(\theta_{GKS}), \tag{10}$$

where η and $\nabla_\theta \mathcal{L}_j(\theta)$ represent the learning rate and partial derivative of parameter θ.

Algorithm 1: Graph-driven feature update

Input: Images $\{I_{si}, i \in (1,m)\}$ of source domain $\mathcal{D}om_s$, and images $\{I_{tj}, j \in (1,n)\}$ of target domain $\mathcal{D}om_t$.

Output: The optimized features $\{f_{si}^{q''}\}$ of the source domain.

for $\{I_{si}, i \in (1,m)\}$ **do**
  $(f_{si}^d, dis_z) = \mathcal{G}_{DC}(I_{si})$.
for $\{I_{tj}, i \in (1,n)\}$ **do**
  $(f_{tj}^d, dis_z) = \mathcal{G}_{DC}(I_{tj})$.
while $dis_z, z \in (1,25)$ **do**
  $e_{i,j} = \mathcal{D}(f_{si}^d, f_{tj}^d)$.
end while
$\mathcal{A}_{st} = \{e_{i,j} | i \in (1,m), j \in (1,n)\}$.
for $\{I_{si}, i \in (1,m)\}$ **do**
  $f_{si}^q = \mathcal{G}_{fex}(I_{si})$.
for $\{I_{tj}, i \in (1,n)\}$ **do**
  $f_{tj}^q = \mathcal{G}_{fex}(I_{tj})$.
$\mathcal{H}_{st} = \{\{f_{si}^q\}, \{f_{tj}^q\} | i \in (1,m), j \in (1,n)\}$.
$/\star\ GKL\ for\ knowledge\ sharing\ \star/$
$\mathcal{H}_{st}^{'} = \sigma(\mathcal{A}_{st}\mathcal{H}_{st}\mathcal{W}_1 + \mathcal{B}_1)$.
$\mathcal{H}_{st}^{''} = \sigma(\mathcal{A}_{st}\mathcal{H}_{st}^{'}\mathcal{W}_2 + \mathcal{B}_2)$.
Obtain updated features $\{f_{si}^{q''}\}$ from $\mathcal{H}_{st}^{''}$.
return $\{f_{si}^{q''}\}$

	Methods *(year)*	LIVEC		KonIQ-10k		BID		Average	
		SRCC	PLCC	SRCC	PLCC	SRCC	PLCC	SRCC	PLCC
Hand-craft methods	BRISQUE *(2012)*	0.243	0.251	0.108	0.099	0.175	0.175	0.175	0.175
	NIQE *(2012)*	0.304	0.362	0.447	0.460	0.355	0.381	0.369	0.401
	PIQE *(2015)*	0.262	0.362	0.084	0.200	0.269	0.351	0.205	0.304
Classic deep-learning methods	RankIQA *(2017)*	0.491	0.495	0.603	0.551	0.510	0.67	0.535	0.471
	MetaIQA *(2020)*	0.464	0.464	0.501	0.504	0.300	0.428	0.422	0.465
	DBCNN *(2023)*	0.266	0.290	0.413	0.421	0.318	0.212	0.332	0.307
	HyperIQA *(2020)*	0.490	0.487	0.545	0.556	0.379	0.282	0.472	0.442
	AKD-IQA *(2025)*	0.372	0.364	0.467	0.477	0.502	0.493	0.447	0.429
	DiffV^2IQA *(2025)*	0.329	0.323	0.498	0.476	0.387	0.366	0.391	0.388
	MCOLE *(2024)*	0.411	0.395	0.472	0.473	0.426	0.418	0.436	0.429
Cross-domain methods	DANN *(2014)*	0.499	0.484	0.638	0.636	0.586	0.510	0.574	0.543
	UCDA *(2021)*	0.382	0.358	0.496	0.501	0.348	0.391	0.408	0.417
	RankDA *(2021)*	0.451	0.455	0.638	0.623	0.535	0.582	0.542	0.553
	StyleAM *(2024)*	0.584	0.561	**0.700**	0.673	0.637	0.567	0.640	0.600
	DGQA *(2024)*	**0.696**	**0.690**	0.681	**0.687**	**0.770**	**0.753**	**0.716**	**0.710**
	Ours	**0.753**	**0.756**	**0.721**	**0.738**	**0.787**	**0.781**	**0.754**	**0.758**

Table 1: Performance comparisons of existing IQA methods in synthetic-to-authentic settings.

After obtaining $\theta^{'}_{IQA}$ with the joint feedback of the CAL framework, the IQA model can suit for the target domain. While meeting target domain from new scenarios, the image I_{tj} is input into IQA model $\mathcal{G}_{IQA}$. The corresponding quality score Q_{tj} is obtained:

$$\{\mathcal{Q}_{tj}\} = \mathcal{G}_{IQA}(\theta^{'}_{IQA}, \{I_{tj}\}), j \in (1, n). \quad (11)$$

Experiments

Experimental Settings

This section includes the expression of datasets, metrics, and parameters details.

Datasets and Metrics. We conducted experiments on 6 natural scenarios datasets, namely, 3 synthetic distortion datasets (KADID (Lin, Hosu, and Saupe 2019), CSIQ (Larson and Chandler 2010), and TID2013 (Ponomarenko et al. 2013)), and 3 authentic distortion datasets (LIVEC (Ghadiyaram and Bovik 2015), BID (Ciancio et al. 2010), and KonIQ-10k (Hosu et al. 2020)). Two AI-generated datasets (AGIQA-3k (Li et al. 2023) and AGIQA-20k (Li et al. 2024b)) and two underwater datasets (SAUD (Jiang et al. 2022) and UIED (Zheng et al. 2022)) were utilized for more cross-domain testing. Two typical metrics, namely, Spearman rank correlation coefficient (SRCC) and Pearson linear correlation coefficient (PLCC), were employed to evaluate the monotonicity and accuracy of the results.

Parameters Details. During training, a random 224×224 patch was sampled from each image, and data augmentation was performed by random horizontal flipping. The RGB features of these patches were input into the quality assessment net. The network was trained with a batch size of 16, and the learning rate η was set to 1×10^{-4}. Additionally, weight decay of the learning rate was applied every 10 epochs, and the weight decay is 0.8. The value of parameters a and b for loss are 0.6 and 0.95 in the baseline.

#	GKS	GLA	CAL	PLCC/SRCC LIVEC	PLCC/SRCC AGIQA-3k
1	✗	✗	✗	0.576/0.582	0.502/0.511
2	✓	✗	✗	0.607/0.593	0. 634/0.631
3	✗	✓	✗	0.607/0.602	0.628/0.617
4	✗	✓	✓	0.654/0.679	0.721/0.723
5	✓	✓	✗	0.624/0.617	0.697/0.691
6	✓	✗	✓	0.730/0.702	0.748/0.735
7	✓	✓	✓	**0.756/0.753**	**0.794/0.781**

Table 2: Effectiveness of GKS, GLA, and CAL.

#	Cross-attention	1DCNN	PLCC/SRCC LIVEC	PLCC/SRCC AGIQA-3k
1	✗	✗	0.730/0.712	0.769/0.762
2	✗	✓	0.741/0.738	0.774/0.769
3	✓	✓	**0.756/0.753**	**0.794/0.781**

Table 3: Effectiveness of cross-attention and 1DCNN.

Performance Comparisons of Synthetic-to-Authentic Tasks

To demonstrate the performance in cross-domain tasks, GDCIQA was compared with 15 IQA methods, including 3 handcrafted methods, namely, BRISQUE (Mittal, Moorthy, and Bovik 2012), NIQE (Mittal, Soundararajan, and Bovik 2012) and PIQE (Venkatanath et al. 2015), 7 classic deep learning-based methods, namely, RankIQA (Liu, Van De Weijer, and Bagdanov 2017), MetaIQA (Zhu et al. 2020), DBCNN (Zhang et al. 2023a), HyperIQA (Su et al. 2020), AKD-IQA (Hu et al. 2025), DiffV^2IQA (Wang et al. 2025), and MCOLE (Jiang et al. 2024), and 5 cross-domain methods, namely, DANN (Ajakan et al. 2014), UCDA (Chen et al. 2021b), RankDA (Chen et al. 2021a), StyleAM (Lu et al. 2024) and DGQA (Li et al. 2024a). Handcrafted methods are compared to validate the advantage of utiliz-

ing deep-learning. Classic deep learning-based methods are compared to validate the significance of addressing cross-domain tasks. Cross-domain methods are compared to validate the advantage of our cross-domain framework. All methods trains on KADID, and then tests on LIVEC, BID and KonIQ-10k, respectively.

The results are illustrated in Table 1 and the best results are in bold. The experimental results demonstrate that the SRCC and PLCC of GDCIQA are at least 8.19% and 9.56% higher than these methods on LIVEC, at least 3.0% and 7.42% higher than these methods on KonIQ-10k, and at least 2.21% and 3.72% higher than these methods on BID, respectively. The average values of the SRCC and PLCC of GDCIQA are also the best. Therefore, GDCIQA perform best in synthetic-to-authentic Tasks.

Ablation Study

This section includes experiments for demonstrating the effectiveness of GKS, GLA, CAL, respectively.

Effectiveness of GKS, GLA, and CAL. To validate the effectiveness of GKS, GLA, and CAL, Table 2 is illustrated. In Table 2, scheme #1 removes all three modules. Scheme #2 and #3 only utilize one of the GKS and GLA, respectively. Scheme #4, #5, and #6 only remove one of the GKS, GLA, and CAL, respectively. The scheme #7 is the baseline of GDCIQA. All schemes are trained on KADID and tested on LIVEC and AGIQA-3K and best results are in bold. The experimental results demonstrate that one of three modules can improve the model by 5.38%, 14.24%, and 5.38% in PLCC, respectively. By utilizing two of three modules can improve the model by at least 8.33% and 6.01% in PLCC and SRCC, respectively. Utilizing all three modules improve the model by 31.25% and 29.38% in PLCC and SRCC, respectively. Therefore, the GKS, GLA, and CAL in GDCIQA are effective in measuring image quality.

Effectiveness of cross-attention and 1DCNN in GLA. To validate the effectiveness of cross-attention and 1DCNN in GLA, Table 3 are illustrated. In Table 3, scheme #1 removes cross-attention and 1DCNN. The scheme #2 only utilizes the 1DCNN and then concats with linear layers. The scheme #3 is the baseline of GDCIQA. All schemes are trained on KADID and tested on LIVEC and AGIQA-3K. The best results are in bold. The experimental results demonstrate that 1DCNN improves the model by 1.51% and 3.65% in PLCC and SRCC, respectively. Based on this, using cross-attention for cross-features can improve the model by 2.02% and 2.03% in PLCC and SRCC, respectively. Therefore, the cross-attention and 1DCNN in GLA are effective in measuring image quality.

Analysis of CAL

To validate the robustness and generalization of the framework of GDCIQA, more deep-learning networks are employed to replace the distortion extractor and feature extractor. Specially, ResNet-50, DenseNet-121, VGG-16, GoogleNet, and Swin Transformer are employed in Figure 3 and Figure 4. Experimental results demonstrate that the performance is higher than existing methods while the feature extractor is ResNet-50 and DenseNet-121. Only DGQA competes with GDCIQA, when the feature extractor of GDCIQA is VGG-16 and GoogleNet. The performance of our model is higher than existing methods while the distortion extractor is replaced. Therefore, extending the CAL framework to more networks is feasible in the future work.

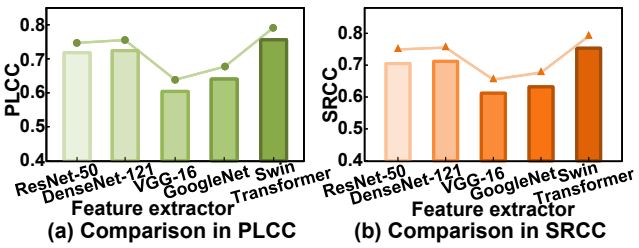

Figure 3: The illustration of results of using different feature extractors in IQA.

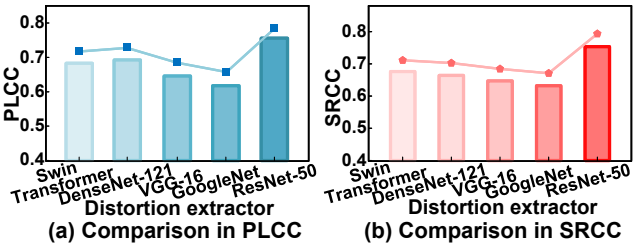

Figure 4: The illustration of results of using different distortion extractors.

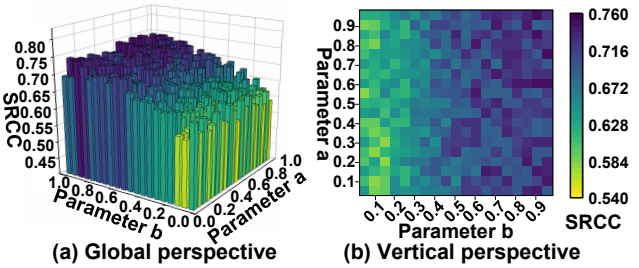

Figure 5: The illustration of results of setting different value of parameter a and b.

Effectiveness of Hyper-parameters

To further analyze the effectiveness of two hyper-parameters a and b in the CAL framework, we tested the model performance while a and b changes. The values of a and b are selected from 0 to 1 with growth step size of 0.05. The SRCC, a, and b are recorded as the z-axis, x-axis, and y-axis, respectively. The three-dimensional column chart is illustrated in Figure 5 (a). Meanwhile, the vertical perspective chart is illustrated in Figure 5 (b). Experimental results demonstrate that the model performance improves while the value of b added. While the value of a is 0.6, the model performance is

	Method	KADID	CSIQ	TID2013
AGIQA -3k	BRISQUE	0.178	0.205	0.148
	DBCNN	0.324	0.427	0.364
	HyperIQA	**0.748**	**0.741**	**0.733**
	MetaIQA	0.468	0.523	0.429
	UCDA	0.681	0.718	0.574
	DGQA	0.577	0.628	0.612
	Ours	**0.781**	**0.764**	**0.741**
AGIQA -20k	BRISQUE	0.118	0.098	0.238
	DBCNN	0.284	0.317	0.268
	HyperIQA	**0.516**	0.411	0.359
	MetaIQA	0.348	0.329	0.415
	UCDA	0.255	0.368	0.397
	DGQA	0.498	**0.526**	**0.512**
	ours	**0.653**	**0.584**	**0.640**

Table 4: Performance comparisons of the existing IQA methods in AI-generated scenarios.

	Method	KADID	CSIQ	TID2013
SAUD	BRISQUE	0.216	0.159	0.243
	DBCNN	0.418	0.351	0.338
	HyperIQA	0.497	0.529	**0.591**
	MetaIQA	0.586	0.510	0.569
	UCDA	0.623	0.527	0.498
	DGQA	**0.627**	**0.531**	0.524
	Ours	**0.679**	**0.617**	**0.652**
UIED	BRISQUE	0.253	0.105	0.117
	DBCNN	0.348	0.271	**0.438**
	HyperIQA	**0.497**	0.325	0.369
	MetaIQA	0.481	0.397	0.329
	UCDA	0.409	0.317	0.358
	DGQA	0.434	**0.401**	0.409
	Ours	**0.566**	**0.462**	**0.458**

Table 5: Performance comparisons of the existing IQA methods in underwater scenarios.

stable with over 0.7 in SRCC. The parameters a and b whose value are 0.6 and 0.95 in our baseline are optimal.

Cross-data Analysis

To prove the performance of GDCIQA in cross-data scenarios, six methods are compared in SRCC in Table 4 and Table 5 are illustrated. 3 natural scenario datasets (KADID, CSIQ, and TID2013) are for training, and 2 AI-generated datasets (AGIQA-3k and AGIQA-20k) and two underwater datasets (SAUD and UIED) are for test. The best two results in Table 4 and Table 5 are in bold. The experimental results demonstrate that, compared to other methods, our method improves by at least 11.03% in AGIQA-20k, improves by at least 8.29% and 4.57% in SAUD and UIED, respectively. Therefore, GDCIQA performs best in cross-data tasks, which meets various IQA scenarios.

Visual Analysis

This section includes visual analysis of domain addressing, accuracy, stability, and convergence rate of GDCIQA.

Analysis of domain addressing. To demonstrate the effectiveness of domain addressing of GDCIQA, several samples are illustrated for visual expression. As illustrated in Figure 6, the edge between the source domain images and target domain images in the same distortion represents the distortion distance. The best and worst edges are green and red, respectively. The results demonstrate that the source domain images is similar to the target domain images.

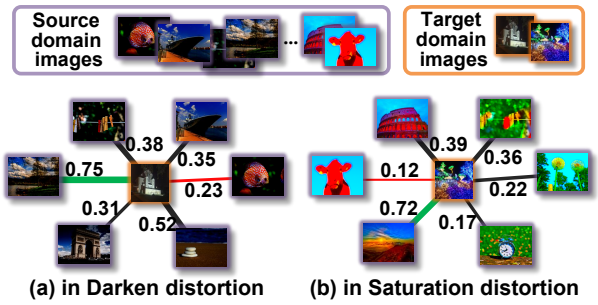

Figure 6: The illustration of graph visual information of several samples.

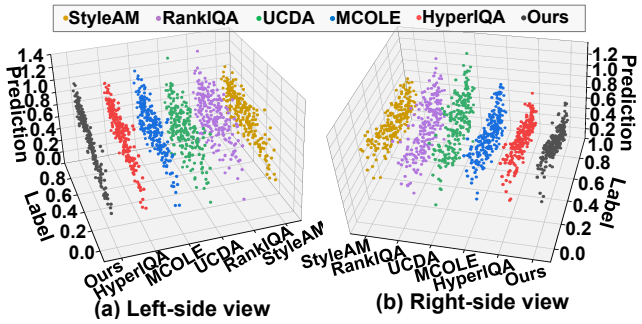

Figure 7: The illustration of performance comparisons.

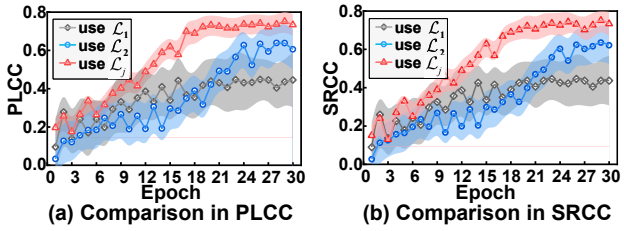

Figure 8: The illustration of stability and convergence rate.

Analysis of accuracy. To demonstrate the accuracy of GDCIQA, the predicted scores obtained by GDCIQA and labels are plotted as black scatters in Figure 7, when LIVEC is for test. The scatters of 5 methods are illustrated for comparisons. The results demonstrate that scatters of GDCIQA is the most concentrated and predicted scores are close to the labels, which demonstrate that GDCIQA is more accurate.

Analysis of stability and convergence rate. To demonstrate the stability and convergence rate of GDCIQA, the SRCC in each epoch are illustrated as red dotted line chart in Figure 8. The changes of SRCC by using only $\mathcal{L}_1$ or $\mathcal{L}_2$ are for comparisons. The error bands of 100 rounds are also added. The results demonstrate that GDCIQA converges with 17 epochs, while using only $\mathcal{L}_1$ and only $\mathcal{L}_2$ converges with 22 epochs and 27 epochs. Moreover, the performance of GDCIQA is at least 19.31% higher than using only $\mathcal{L}_1$ or $\mathcal{L}_2$, while with more stable error. These jointly demonstrate the better stability and faster convergence rate of GDCIQA.

Conclusion

This paper proposes a graph-driven domain co-adaptation framework for cross-domain IQA tasks. Firstly, a GKS module is designed for knowledge sharing by quality-aware and distortion-related information. Secondly, a CAL mechanism is proposed for feeding back the model to joint optimize the different modules. Finally, a domain adaptation framework has been designed to train models on labeled source images, yielding target-domain-optimized IQA models. Experimental results demonstrate that GDCIQA achieves higher accuracy and stability in cross-domain scenarios.

In future work, we will consider more perspectives for the knowledge sharing between the source domain and the target domain. Moreover, considering the maturity of the large model, it can be suitable for image correlation analysis. Therefore, the large model will be employed in our novel cross-domain IQA method to address the complex requirements of real-world applications.

Acknowledgments

This work was supported by the National Natural Science Foundation of China (Grant No. 62101268, 82204770, 62472226), and the Open Project Program of the State Key Laboratory of CAD&CG (Grant No. A2519), Zhejiang University.

References

Agnolucci, L.; Galteri, L.; Bertini, M.; and Del Bimbo, A. 2024. Arniqa: Learning distortion manifold for image quality assessment. In *Proceedings of the IEEE/CVF Winter Conference on Applications of Computer Vision*, 189–198.

Ajakan, H.; Germain, P.; Larochelle, H.; Laviolette, F.; and Marchand, M. 2014. Domain-adversarial neural networks. *arXiv preprint arXiv:1412.4446*.

Chen, B.; Li, H.; Fan, H.; and Wang, S. 2021a. No-reference screen content image quality assessment with unsupervised domain adaptation. *IEEE Transactions on Image Processing*, 30: 5463–5476.

Chen, P.; Li, L.; Wu, J.; Dong, W.; and Shi, G. 2021b. Unsupervised curriculum domain adaptation for no-reference video quality assessment. In *Proceedings of the IEEE/CVF International Conference on Computer Vision*, 5178–5187.

Cheng, K.; Liu, Y.; and Zeng, X. 2023. Learning graph enhanced spatial-temporal coherence for video anomaly detection. *IEEE Signal Processing Letters*, 30: 314–318.

Ciancio, A.; da Silva, E. A.; Said, A.; Samadani, R.; Obrador, P.; et al. 2010. No-reference blur assessment of digital pictures based on multifeature classifiers. *IEEE Transactions on Image Processing*, 20(1): 64–75.

Fang, X.; Chen, P.; Wang, M.; and Wang, S. 2025. Examining the role of compression in influencing AI-generated image authenticity. *Scientific Reports*, 15(1): 12192.

Fang, Y.; Zhang, Q.; Zhang, N.; Chen, Z.; Zhuang, X.; Shao, X.; Fan, X.; and Chen, H. 2023. Knowledge graph-enhanced molecular contrastive learning with functional prompt. *Nature Machine Intelligence*, 5(5): 542–553.

Ghadiyaram, D.; and Bovik, A. C. 2015. Massive online crowdsourced study of subjective and objective picture quality. *IEEE Transactions on Image Processing*, 25(1): 372–387.

Guan, J.; Yi, S.; Zeng, X.; Cham, W.-K.; and Wang, X. 2017. Visual importance and distortion guided deep image quality assessment framework. *IEEE Transactions on Multimedia*, 19(11): 2505–2520.

Hosu, V.; Lin, H.; Sziranyi, T.; and Saupe, D. 2020. KonIQ-10k: An ecologically valid database for deep learning of blind image quality assessment. *IEEE Transactions on Image Processing*, 29: 4041–4056.

Hu, B.; Chen, W.; Zheng, J.; Li, L.; Lu, W.; and Gao, X. 2025. No-Reference Image Quality Assessment via Inter-Level Adaptive Knowledge Distillation. *IEEE Transactions on Broadcasting*.

Hu, B.; Zhu, G.; Li, L.; Gan, J.; Li, W.; and Gao, X. 2023. Blind image quality index with cross-domain interaction and cross-scale integration. *IEEE Transactions on Multimedia*.

Im, J.; Nam, J.; Park, N.; Lee, H.; and Park, S. 2024. Egtr: Extracting graph from transformer for scene graph generation. In *Proceedings of the IEEE/CVF Conference on Computer Vision and Pattern Recognition*, 24229–24238.

Jiang, Q.; Gu, Y.; Li, C.; Cong, R.; and Shao, F. 2022. Underwater image enhancement quality evaluation: Benchmark dataset and objective metric. *IEEE Transactions on Circuits and Systems for Video Technology*, 32(9): 5959–5974.

Jiang, Q.; Yi, X.; Ouyang, L.; Zhou, J.; and Wang, Z. 2024. Towards dimension-enriched underwater image quality assessment. *IEEE Transactions on Circuits and Systems for Video Technology*.

Jin, M.; Koh, H. Y.; Wen, Q.; Zambon, D.; Alippi, C.; Webb, G. I.; King, I.; and Pan, S. 2024. A survey on graph neural networks for time series: Forecasting, classification, imputation, and anomaly detection. *IEEE Transactions on Pattern Analysis and Machine Intelligence*.

Ke, J.; Wang, Q.; Wang, Y.; Milanfar, P.; and Yang, F. 2021. Musiq: Multi-scale image quality transformer. In *Proceedings of the IEEE/CVF International Conference on Computer Vision*, 5148–5157.

Larson, E. C.; and Chandler, D. M. 2010. Most apparent distortion: full-reference image quality assessment and the role of strategy. *Journal of Electronic Imaging*, 19(1): 011006–011006.

Li, A.; Wu, J.; Liu, Y.; and Li, L. 2024a. Bridging the Synthetic-to-Authentic Gap: Distortion-Guided Unsupervised Domain Adaptation for Blind Image Quality Assessment. In *Proceedings of the IEEE/CVF Conference on Computer Vision and Pattern Recognition*, 28422–28431.

Li, C.; Guo, C.; Ren, W.; Cong, R.; Hou, J.; Kwong, S.; and Tao, D. 2019. An underwater image enhancement benchmark dataset and beyond. *IEEE Transactions on Image Processing*, 29: 4376–4389.

Li, C.; Kou, T.; Gao, Y.; Cao, Y.; Sun, W.; Zhang, Z.; Zhou, Y.; Zhang, Z.; Zhang, W.; Wu, H.; et al. 2024b. Aigiqa-20k: A large database for ai-generated image quality assessment. In *Proceedings of the IEEE/CVF Conference on Computer Vision and Pattern Recognition*, 6327–6336.

Li, C.; Zhang, Z.; Wu, H.; Sun, W.; Min, X.; Liu, X.; Zhai, G.; and Lin, W. 2023. Agiqa-3k: An open database for ai-generated image quality assessment. *IEEE Transactions on Circuits and Systems for Video Technology*.

Li, W.; Wang, J.; Gao, Y.; Zhang, M.; Tao, R.; and Zhang, B. 2022. Graph-feature-enhanced selective assignment network for hyperspectral and multispectral data classification. *IEEE Transactions on Geoscience and Remote Sensing*, 60: 1–14.

Lin, H.; Hosu, V.; and Saupe, D. 2019. KADID-10k: A large-scale artificially distorted IQA database. In *2019 Eleventh International Conference on Quality of Multimedia Experience (QoMEX)*, 1–3. IEEE.

Liu, J.; Li, X.; An, S.; and Chen, Z. 2022. Source-free unsupervised domain adaptation for blind image quality assessment. *arXiv preprint arXiv:2207.08124*.

Liu, X.; Van De Weijer, J.; and Bagdanov, A. D. 2017. Rankiqa: Learning from rankings for no-reference image quality assessment. In *Proceedings of the IEEE International Conference on Computer Vision*, 1040–1049.

Liu, Z.; Lin, Y.; Cao, Y.; Hu, H.; Wei, Y.; Zhang, Z.; Lin, S.; and Guo, B. 2021. Swin transformer: Hierarchical vision transformer using shifted windows. In *Proceedings of the IEEE/CVF International Conference on Computer Vision*, 10012–10022.

Lu, Y.; Li, X.; Liu, J.; and Chen, Z. 2024. StyleAM: Perception-Oriented Unsupervised Domain Adaption for No-reference Image Quality Assessment. *IEEE Transactions on Multimedia*.

Min, X.; Gao, Y.; Cao, Y.; Zhai, G.; Zhang, W.; Sun, H.; and Chen, C. W. 2025. Exploring rich subjective quality information for image quality assessment in the wild. *IEEE Transactions on Circuits and Systems for Video Technology*.

Mittal, A.; Moorthy, A. K.; and Bovik, A. C. 2012. No-reference image quality assessment in the spatial domain. *IEEE Transactions on Image Processing*, 21(12): 4695–4708.

Mittal, A.; Soundararajan, R.; and Bovik, A. C. 2012. Making a "completely blind" image quality analyzer. *IEEE Signal Processing Letters*, 20(3): 209–212.

Ou, F.-Z.; Chen, X.; Zhang, R.; Huang, Y.; Li, S.; Li, J.; Li, Y.; Cao, L.; and Wang, Y.-G. 2021. SDD-FIQA: Unsupervised face image quality assessment with similarity distribution distance. In *Proceedings of the IEEE/CVF Conference on Computer Vision and Pattern Recognition*, 7670–7679.

Ponomarenko, N.; Ieremeiev, O.; Lukin, V.; Egiazarian, K.; Jin, L.; Astola, J.; Vozel, B.; Chehdi, K.; Carli, M.; Battisti, F.; et al. 2013. Color image database TID2013: Peculiarities and preliminary results. In *European workshop on Visual Information Processing (EUVIP)*, 106–111. IEEE.

Su, S.; Yan, Q.; Zhu, Y.; Zhang, C.; Ge, X.; Sun, J.; and Zhang, Y. 2020. Blindly assess image quality in the wild guided by a self-adaptive hyper network. In *Proceedings of the IEEE/CVF Conference on Computer Vision and Pattern Recognition*, 3667–3676.

Sun, S.; Yu, T.; Xu, J.; Zhou, W.; and Chen, Z. 2022. GraphIQA: Learning distortion graph representations for blind image quality assessment. *IEEE Transactions on Multimedia*, 25: 2912–2925.

Targ, S.; Almeida, D.; and Lyman, K. 2016. Resnet in resnet: Generalizing residual architectures. *arXiv preprint arXiv:1603.08029*.

Venkatanath, N.; Praneeth, D.; Bh, M. C.; Channappayya, S. S.; and Medasani, S. S. 2015. Blind image quality evaluation using perception based features. In *2015 twenty first National Conference on Communications (NCC)*, 1–6. IEEE.

Wang, Y.; Luo, X.; Chen, C.; Hua, X.-S.; Zhang, M.; and Ju, W. 2024. DisenSemi: Semi-supervised graph classification via disentangled representation learning. *IEEE Transactions on Neural Networks and Learning Systems*.

Wang, Z.; Hu, B.; Zhang, M.; Li, J.; Li, L.; Gong, M.; and Gao, X. 2025. Diffusion Model-Based Visual Compensation Guidance and Visual Difference Analysis for No-Reference Image Quality Assessment. *IEEE Transactions on Image Processing*.

Wei, Y.; Fu, S.; Jiang, W.; Zhang, Z.; Zeng, Z.; Wu, Q.; Kwok, J.; and Zhang, Y. 2024. Gita: Graph to visual and textual integration for vision-language graph reasoning. *Advances in Neural Information Processing Systems*, 37: 44–72.

Yang, K.; Xu, Y.; Zou, P.; Ding, H.; Zhao, J.; Wang, Y.; and Xie, B. 2023. KerPrint: local-global knowledge graph enhanced diagnosis prediction for retrospective and prospective interpretations. In *Proceedings of the AAAI Conference on Artificial Intelligence*, volume 37, 5357–5365.

Yang, L.; Chen, H.; Li, Z.; Ding, X.; and Wu, X. 2024. Give us the facts: Enhancing large language models with knowledge graphs for fact-aware language modeling. *IEEE Transactions on Knowledge and Data Engineering*, 36(7): 3091–3110.

Yang, L.; Chen, X.; Zhuo, J.; Jin, D.; Wang, C.; Cao, X.; Wang, Z.; and Guo, Y. 2025. Disentangled Graph Spectral Domain Adaptation. In *Forty-second International Conference on Machine Learning*.

Yu, Y.; Xia, S.; Lin, X.; Yang, W.; Lu, S.; Tan, Y.-P.; and Kot, A. 2025. Backdoor attacks against no-reference image quality assessment models via a scalable trigger. In *Proceedings of the AAAI Conference on Artificial Intelligence*, volume 39, 9698–9706.

Zhang, W.; Ma, K.; Zhai, G.; and Yang, X. 2024. Task-specific normalization for continual learning of blind image quality models. *IEEE Transactions on Image Processing*.

Zhang, W.; Zhai, G.; Wei, Y.; Yang, X.; and Ma, K. 2023a. Blind image quality assessment via vision-language correspondence: A multitask learning perspective. In *Proceedings of the IEEE/CVF Conference on Computer Vision and Pattern Recognition*, 14071–14081.

Zhang, Y. 2025. Social Network User Profiling for Anomaly Detection Based on Graph Neural Networks. In *2025 5th International Conference on Artificial Intelligence and Industrial Technology Applications (AIITA)*, 1197–1201. IEEE.

Zhang, Y.; Zhu, H.; Song, Z.; Koniusz, P.; and King, I. 2023b. Spectral feature augmentation for graph contrastive learning and beyond. In *Proceedings of the AAAI Conference on Artificial Intelligence*, volume 37, 11289–11297.

Zheng, Y.; Chen, W.; Lin, R.; Zhao, T.; and Le Callet, P. 2022. UIF: An objective quality assessment for underwater image enhancement. *IEEE Transactions on Image Processing*, 31: 5456–5468.

Zhu, H.; Li, L.; Wu, J.; Dong, W.; and Shi, G. 2020. MetaIQA: Deep meta-learning for no-reference image quality assessment. In *Proceedings of the IEEE/CVF Conference on Computer Vision and Pattern Recognition*, 14143–14152.

Zhuo, J.; Liu, Y.; Lu, Y.; Ma, Z.; Fu, K.; Wang, C.; Guo, Y.; Wang, Z.; Cao, X.; and Yang, L. 2025a. DUALFormer: Dual Graph Transformer. In *The Thirteenth International Conference on Learning Representations*.

Zhuo, J.; Ma, Z.; Lu, Y.; Liu, Y.; Fu, K.; Jin, D.; Wang, C.; Wu, W.; Wang, Z.; Cao, X.; and Yang, L. 2025b. A Closer Look at Graph Transformers: Cross-Aggregation and Beyond. In *The Thirty-ninth Annual Conference on Neural Information Processing Systems*.